Volume 1 | Number 1 | Jan 2013 | Pages 1–100

ChemComm

Chemical Communications
www.rsc.org/chemcomm

ROYAL SOCIETY OF CHEMISTRY

ROYAL SOCIETY OF CHEMISTRY

www.rsc.org/chemcomm

Journal Name

COMMUNICATION

Matrix-free synthesis of spin crossover micro-rods showing large hysteresis loop centered at room temperature

Haonan Peng, Gábor Molnár, Lionel Salmon,* Azzedine Bousseksou*

An original simple homogeneous acid medium was used to synthesize polymer/surfactant-free acicular micro-rod particles (10-40 μm long by 0.1-0.3 μm diameter) of the novel [Fe(Htrz)$_3$](CF$_3$SO$_3$)$_2$ complex. The study of the spin crossover properties reveals a rare 50 K hysteretic behavior perfectly centered at room temperature accompanied by a pronounced thermochromism effect, purple in the low spin state and white in the high spin state.

In order to constitute high-density storage memory device, the use of single molecular or molecular assembly for information processing becomes a very appealing research topic.[1-4] One of the most spectacular examples is the spin-crossover (SCO) phenomenon, which occurs between d^4 - d^7 transition metal complexes wherein the spin state of the metal center changes due to external stimuli such as a variation of temperature, pressure, light irradiation or an influence of a magnetic field.[5] However, one of the still relevant great challenges underlying the spin crossover materials for memory device application notably is to produce controlled size systems[6] that exhibit properties at room temperature and with large hysteresis loop.[7] So far, although the first spin crossover material was reported in 1931,[8] the pioneering example showing bistability at room temperature was reported only in 1993.[9] In this work, the authors controlled the spin transition temperature by mixing of 4-NH$_2$trz and Htrz ligands (trz = triazole), and obtained the complex {[Fe(Htrz)$_{2.85}$(4-NH$_2$trz)$_{0.15}$]}(ClO$_4$)$_2$ exhibiting a hysteresis loop of 16 K centred at 296 K. Up to now only four other bulk compounds presenting such behavior have been reported. Similar [Fe(NH$_2$trz)$_3$](NO$_3$)$_{1.7}$(BF$_4$)$_{0.3}$ complex was also synthesized by mixing two counteranions revealing a 60 K hysteresis loop centred at 310 K.[3] In 2001, the dehydrated form of the Hofmann like clathrate coordination network [Fe(pz){Pt(CN)$_4$}] (pz = pyrazine) presenting a 25 K wide hysteresis loop centered at 290 K was reported.[10] The

corresponding bpac (bis(4-pyridyl)acetylene) derivative exhibits hysteresis loop of 49 K (T$_{1/2(\downarrow)}$ = 251 K and T$_{1/2(\uparrow)}$ = 300 K)[11]. More recently, the first molecular iron(II) complex [Fe(Ph(Imoxo)$_2$)(HIm)$_2$] (Ph(Imoxo)$_2$ = diethyl(E,E)-2,2'-[1,2-phenylenebis-(iminomethylidyne)]-bis[3-butanoate], HIm = imidazole) was shown to exhibit an abrupt spin transition centred at approximately 297 K (T$_{1/2(\downarrow)}$ = 244 K and T$_{1/2(\uparrow)}$ = 314 K).[12] Although hysteretic spin crossover at room temperature is a prerequisite to go toward several applications such as inkless paper,[13] display[3] and memory, the possibility to obtain regular and organized nano- and micro objects is also crucial. It has been shown that the elaboration of thin film[14,15] or nano- and microparticles[16-18] of the SCO clathrate (bpac and pz derivatives) leads to the decrease of the abrupt character of the transitions and also to the modification of the bistability temperatures out of the more suitable temperatures. In the present study, we report on an original homogeneous medium method to obtain regular rod shaped particles of the new [Fe(Htrz)$_3$](CF$_3$SO$_3$)$_2$ complex with very favorable bistability maintained at room temperature.
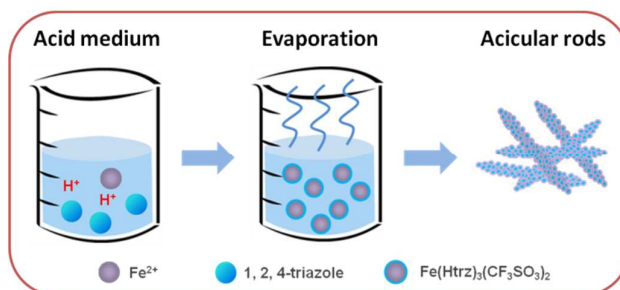
Scheme 1: Elaboration of the [Fe(Htrz)$_3$](CF$_3$SO$_3$)$_2$ microrods in homogeneous acid condition

[Fe(Htrz)$_3$](CF$_3$SO$_3$)$_2$ complex was synthesized simply mixing at room temperature Fe(CF$_3$SO$_3$)$_2$ salt and Htrz (1,2,4-triazole) ligand in acid aqueous medium (in presence of CF$_3$SO$_3$H) without any stabilizing agent (polymer, surfactant). After *ca.* 2 months and a controlled evaporation speed of the solvent, crystalline powder sample of the [Fe(Htrz)$_3$](CF$_3$SO$_3$)$_2$·1.2H$_2$O (**1**) derivative was obtained (see SI for the detailed synthesis). The composition of the samples was

Laboratoire de Chimie de Coordination, CNRS UPR-8241 and Université de Toulouse ; UPS, INP ; F-31077 Toulouse, France. E-mail: lionel.salmon@lcc-toulouse.fr; Azzedine.Bousseksou@lcc-toulouse.fr.
† Electronic Supplementary Information (ESI) available. See DOI: 10.1039/x0xx00000x

obtained thanks to combined thermogravimetric, elemental and EDX (Energy Dispersive X-Ray) analyses (see the experimental section in ESI). It is interesting to notice that in contrast with the Fe/1,2,4-triazole/BF$_4$ derivative[19] all the tentative experiments using different solvents and without the addition of the triflic acid led inexorably to the [Fe(Htrz)$_2$(trz)](CF$_3$SO$_3$) (**2**) derivative and not to the fully protonated ligand sample **1**. Infrared spectra of sample **1** and **2** are shown in ESI. Clearly, sample **2** exhibits spectrum corresponding to the composition [Fe(Htrz)(trz)](CF$_3$SO$_3$) with in particular vibrational modes at 1515 and 1499 cm^{-1} which can be attributed to the stretching deformation of the protonated and unprotonated ligands, respectively. In contrast IR spectrum of sample **1** obtained in presence of acid presents different features in this area with the disappearance of the vibrational mode at 1515 cm^{-1}. Moreover, the presence of a broad peak around 3600 cm^{-1} characteristic of the presence of water confirms the proposed formula. Powder X-ray diffraction (PXRD) patterns were also recorded for samples **1** and **2**. The patterns observed for the two samples have similarities with those measured for the BF$_4$ derivatives. X-ray diffraction allows also for the estimation of the crystallite size using the Scherrer equation. The average crystallite size for both samples was measured at about 80 nm. In this family of "Fe-triazole" coordination polymer, single crystals XRD are very difficult to obtain.[20]

Transmission electronic microscopy (TEM), scanning electronic microscopy (SEM) and high resolution electronic microscopy coupled quantified energy dispersive X-ray spectroscopy analyses (HRTEM EDX) were used to determine the shape, the size and to confirm the composition of the particles. Figure 1 presents representative images for sample **1**. See also ESI for complementary images. Sample **1** displays morphology forming acicular rods with length ranging from 10 to 40 μm, and diameter from 0.1 to 0.3 μm. As expected, the EDX analyses show the presence of Fe, S and F atoms.
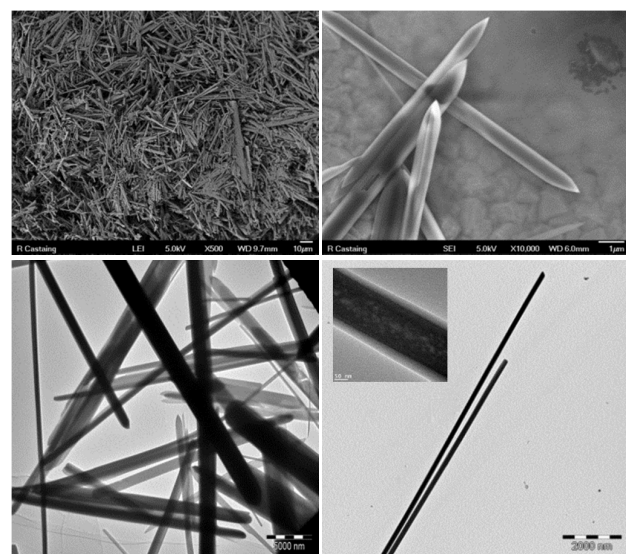

Figure 1: Morphological characterization: SEM (up), TEM (bottom right) and HRTEM (bottom left) images of sample **1**.

Raman spectra were acquired for sample **1** at selected temperatures (Figure 2). These Raman spectra compare well with those reported for compounds of this family.[21] In the considered region of spectra, the spectral features around 100-300 cm^{-1} and 1000-1600 cm^{-1} assigned to metal-ligand stretching and internal ligand modes, respectively, can be identified as spin state markers. In particular, the LS marker bands are found at *ca.* 142, 208, 286, 1042, 1067 and 1083 cm^{-1}, and lower frequency HS marker bands at *ca.* 115, 142, 202, 1037 and 1067 cm^{-1}. Meanwhile, we also measured the Raman spectra at 300 K during both the cooling and
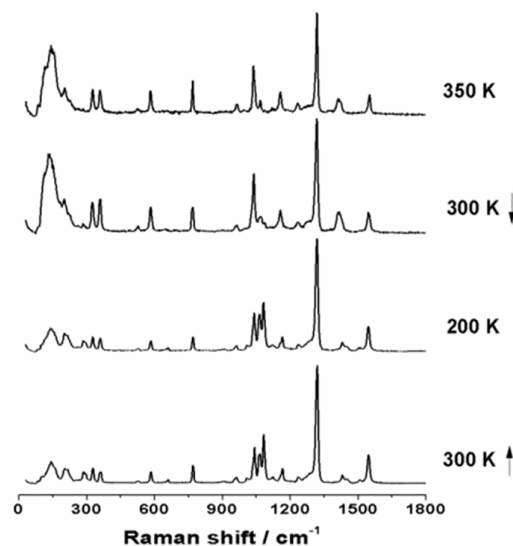
heating process which revealed the room temperature bistability.
Figure 2: Structural characterization: Raman spectra of sample **1** at selected temperatures.

In order to better probe the SCO behavior, the thermal variation of the magnetic susceptibility was investigated for both samples. Concerning sample **2**, these measurements revealed a rather low temperature SCO behavior compared to other compounds of this family[22] with T$_{1/2(\downarrow)}$ ≈ 154 K and T$_{1/2(\uparrow)}$ ≈ 160 K for the hydrated form and T$_{1/2(\downarrow)}$ ≈ 162 K and T$_{1/2(\uparrow)}$ ≈ 166 K for the dehydrated forms. For sample **1**, the first thermal cycle was performed between 100 and 330 K and corresponds to the hydrated form of the sample which presents abrupt spin transition in both the warming and cooling modes (see ESI). The transition temperatures are found at T$_{1/2(\downarrow)}$ ≈ 182 K and T$_{1/2(\uparrow)}$ ≈ 190 K. Following a preliminary thermal treatment at 400 K during 1 hours for dehydration, the second thermal cycle was performed between 100 and 380 K (Figure 3). The transition temperatures are found at T$_{1/2(\downarrow)}$ ≈ 278 K and T$_{1/2(\uparrow)}$ ≈ 327 K, revealing a large hysteresis loop of 50 K perfectly centered at room temperature.

Complementary to the magnetic investigation and due to the drastic color change of the sample from purple to colorless accompanying the spin transition while going from the LS to the HS state, it is obviously interesting to study also the optical behavior of the compound in the visible range (see ESI). The thermal variation of the reflectance (T$_{1/2(\downarrow)}$ ≈ 172 K and T$_{1/2(\uparrow)}$ ≈ 182 K for the hydrated and T$_{1/2(\downarrow)}$ ≈ 283 K and T$_{1/2(\uparrow)}$ ≈ 316 K for the dehydrated sample **1**) compares well with the magnetic results; the slight

　　COMMUNICATION

deviation of the transition temperature being due to the difference of the heating and cooling rates. Using this optical method, it was also possible to control that the SCO properties remains unaltered upon a dozen of thermal cycles (see ESI).
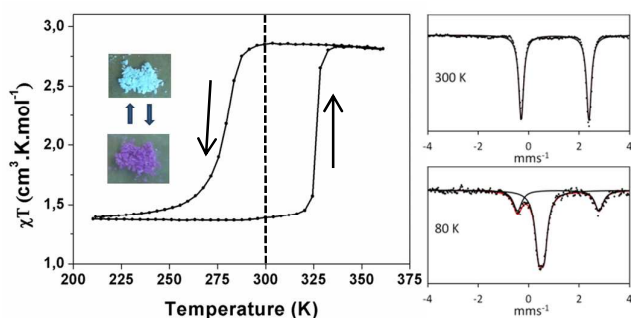

Figure 3: SCO properties: Mössbauer and magnetic (heating/cooling rate = 2 k/min) measurements of dehydrated sample **1** (the insert shows the associated color change of the sample from purple (LS state) to white (HS state)).

The DSC curves were also recorded in the heating and cooling modes at 5 K/min in order to evaluate the enthalpy (ΔH) and entropy (ΔS) variations associated with the spin transition of sample **1** (see ESI). Respectively, the DSC curves show singularities at $T_{1/2(\downarrow)}$ ≈ 173 K and $T_{1/2(\uparrow)}$ ≈ 185 K for hydrated sample and at $T_{1/2(\downarrow)}$ ≈ 290 K and $T_{1/2(\uparrow)}$ ≈ 321 K for dehydrated sample. The estimated ΔH and ΔS associated with the SCO are 12 KJ/mol and 43 J/mol·K, respectively, when corrected by the residual HS fraction at low temperature.

With the aim to determine more precisely the fraction of iron centres involved in the spin transition and to explain the slightly high magnetic susceptibility value measured at low temperature, [57]Fe Mössbauer spectra were recorded for sample **1** at different temperatures (see ESI). As expected, at 300 K the spectrum consists of one doublet with an isomeric shift of 1.049 mms[-1] and a quadrupole splitting of 2.684 mms[-1] attributed to the HS state. Inversely, two doublets with isomeric shift of 0.461 (1.090) mms[-1] and a quadrupole splitting of 0.226 (2.831) mms[-1] attributed to the LS (HS) state are observed at 240 and 80 K, in agreement with the magnetic data of its dehydrated form. The remaining 30% HS fraction at low temperature might be explained by the strong anisotropic morphology of the particles and the concomitant increase of the iron center portion localized at the surface which are possibly spin crossover inactive.

In conclusion, an original homogeneous acid condition was used for the elaboration of highly anisotropic acicular rods of the novel [Fe(Htrz)$_3$](CF$_3$SO$_3$)$_2$ complex. Syntheses in absence of acid conditions allowed us to stabilize only bulk samples of the [Fe(Htrz)$_2$(trz)](CF$_3$SO$_3$) derivative. Compared to the previously reported encapsulating approaches to obtain SCO nano- and micro-objects like the reverse micelles technic [23,24] or methods consisting to use additional polymer as stabilizing agent,[25] the particularity of such approach is to obtain directly regular shape surfactant/polymer-free particles. In fact, the presence of acid in the reaction medium which preclude the deprotonation of the Htrz ligand associated with a controlled slow evaporation speed of the complex solution lead to the slow stabilization of the

[Fe(Htrz)$_3$](CF$_3$SO$_3$)$_2$ long rod-shaped particles. In contrast to the [Fe(Htrz)$_2$(trz)](CF$_3$SO$_3$) form which presents a low temperature SCO behavior compared to other compounds of this family[21] with $T_{1/2(\downarrow)}$ ≈ 162 K and $T_{1/2(\uparrow)}$ ≈ 166 K for the dehydrated forms, the [Fe(Htrz)$_3$](CF$_3$SO$_3$)$_2$ derivative exhibits a rare 50 K hysteretic spin crossover perfectly centered at room temperature. Ultimately, these simple experiments led to the elaboration of already shaped spin crossover objects with very appealing properties. These findings could be surely beneficial for fundamental and applied reasons. In particular, these very high aspect ratio bistable objects could be really useful by means of soft lithographic capillary assembling technic or dielectrophoresis in the competition for the understanding of the spatio-temporal behaviors and also for the transport measurements and switching of organized individual objects which constitute one of the foremost paradigms in molecular electronics. Moreover, the measured largest "real" room temperature bistability reported for such shaped SCO objects is very promising for practical application in the fields of memory devices, display devices, inkless paper and MEMS (Micro Electro Mechanical Systems).[26]

Notes and references

1 J. E. Green, J. Wook Choi, A. Boukai, Y. Bunimovich, E. Johnston-Halperin, E. DeIonno, Y. Luo, B. A. Sheriff, K. Xu, Y. Shik Shin, H. -R. Tseng and J. F. Stoddart, J. R. Heath, *Nature*, 2007, **445**, 414-417.
2 M. Ratner, *Nature Nanotechnology*, 2013, **8**, 378–381.
3 O. Kahn and C. Jay Martinez, *Science*, 1998, **279**, 44-48.
4 A. Bousseksou, G. Molnár, P. Demont and J. Menegotto, *J. Mater. Chem.*, 2003, **13**, 2069-2071.
5 (a) Spin Crossover in Transition Metal Compounds: *Topics in Current Chemistry*, Eds: Gütlich, P. and Goodwin, H. A. Springer, Berlin, 2004, (b) M. Carmen Munoz and J. A. Real, *Coord. Chem. Rev.*, 2011, **255**, 2068, (c) P. Gütlich, A. B. Gaspar and Y. Garcia, *Beilstein J. Org. Chem.* 2013, **9**, 342–391.
6 (a) A. Bousseksou, G. Molnár, L. Salmon and W. Nicolazzi, *Chem. Soc. Rev.* 2011, **40**, 3313, (b) H. J. Shepherd, G. Molnár, W. Nicolazzi, L. Salmon and A. Bousseksou, *Eur. J. Inorg. Chem.* 2013, 653, (c) C. M. Quintero, G. Félix, I. Suleimanov, J. Sánchez Costa, G. Molnár, L. Salmon, W. Nicolazzi and A. Bousseksou, *Beilstein J. Nanotechnol.* 2014, **5**, 2230, (d) G. Molnar, L. Salmon, W. Nicolazzi, F. Terki and A. Bousseksou, *J. Mater. Chem. C*, 2014, **2**, 1360–1366.
7 I. Salitros, N. T. Madhu, R. Boca, J. Pavlik and M. Ruben, *Monatsh. Chem.*, 2009, **140**, 695.
8 L. Cambi and L. Szego, Ber. Drsch. *Chem. Ges. B*, 1931, **64**, 259
9 J. Kröber, E. Codjovi, O. Kahn, F. Grolière and C. Jay, *J. Am. Chem. Soc*, 1993, **115**, 9810.
10 V. Niel, J. M. Martinez-Agudo, M. Carmen Munoz, A. Belen Gaspar and J. Antonio Real, *Inorg. Chem.* 2001, **40**, 3838-3839.
11 C. Bartual-Murgui, N. A. Ortega-Villar, H. J. Shepherd, M. Carmen Munoz, L. Salmon, G. Molnár, A. Bousseksou and J. A. Real, *J. Mater. Chem.*, 2011, **21**, 7217-7222.
12 B. Weber, W. Bauer and J. Obel, *Angew. Chem. Int. Ed.* 2008, **47**, 10098.
13 V. Nagy, I. Suleimanov, G. Molnár, L. Salmon, A. Bousseksou and L. Csóka, *ACS Appl. Mater. Interfaces*, 2015, submitted.

14 S. Cobo, G. Molnár, J. A. Real and A. Bousseksou, *Angew. Chem. Int. Ed.* 2006, **45**, 5786 -5789.

15 C. Bartual-Murgui, A. Akou, L. Salmon, G. Molnár , C. Thibault, J. A. Real and A. Bousseksou, *Small*, 2011, **7**, 23, 3385-3391.

16 I. Boldog, A. B. Gaspar, V. Martinez, P. Pardo-Ibanez, V. Ksenofontov, A. Bhattacharjee, P. Gutlich and J. A. Real, *Angew. Chem. Int. Ed*, 2008, **47**, 6433-6437.

17 F. Volatron, L. Catala, E. Rivière, A. Gloter, O. Stéphan and T. Mallah, *Inorg. Chem.*, 2008, **47**, 15.

18 H. Peng, S. Tricard, G. Félix, G. Molar, W. Nicolazzi, L. Salmon and A. Bousseksou, *Angew. Chem. Int. Ed*. 2014, **53**, 10894.

19 J. Kröber, J. P. Audière, R. Claude, E. Codjovi, O. Kahn, J. G. Hasnoot, F. Grolière, C. Jay, A. Bousseksou, J. Linares, F. Varret and A. Gonthier-Vassal, *Chem. Mater.*, 1994, **6**, 1404.

20 A. Grosjean, N. Daro, B. Kauffmann, A. Kaiba, J.- F. Létard and P. Guionneau, *Chem. Commun.*, 2013, 796.

21 N. Ould Moussa, D. Ostrovskii, V. M. Garcia, G. Molnár, K. Tanaka, A. B. Gaspar, J. A. Real and A. Bousseksou, *Chem. Phys. Lett.*, 2009, **477**, 156-159.

22 O. Roubeau, Chem. Eur. J. 2012, 18, 15230-15244.

23 T. Forestier, S. Mornet, N. Daro, T. Nishihara,S. Mouri, K. Tanaka, O. Fouché, E. Freysz and J.-F. Létard, *Chem. Commun.* 2008, 4327-4329.

24 A. Tokarev, L. Salmon, Y. Guari, G. Molnár and A. Bousseksou, *New J. Chem.* 2011, **35**, 2081-2088.

25 I. Guralskyi, C. M. Quintero, G. Molnár, I. O. Fritsky, L. Salmon and A. Bousseksou, *Chem. A Eur. J.*, 2012, **18**, 9946-9954.

26 H. J. Shepherd, I. A. Gural'skiy, C. M. Quintero, S. Tricard, L. Salmon, G. Molnar and A. Bousseksou, *Nat. Commun.*, 2013, **4**, 2607.